RSC Advances

PAPER

View Article Online
View Journal | View Issue

Cite this: *RSC Adv.*, 2023, **13**, 7425

Gold nanoclusters Cys-Au NCs as selective fluorescent probes for "on–off–on" detection of Fe^{3+} and ascorbic acid†

Wenjie Luo,‡[a] Changxu Wang,‡[b] Jieshu Min[a] and Huiyu Luo *[c]

Gold nanoclusters exhibit attractive properties owing to their excellent biocompatibility and strong photostability in the biomedical domain. In this research, cysteine-protected fluorescent gold nanoclusters (Cys-Au NCs) were synthesized *via* decomposing Au(I)–thiolate complexes for the detection of Fe^{3+} and ascorbic acid in a bidirectional "on–off–on" mode. Meanwhile, the detailed characterization confirmed that the mean particle size of the prepared fluorescent probe was 2.43 nm and showed a fluorescence quantum yield of 3.31%. In addition, our results indicate that the fluorescence probe for ferric ions exhibited a broad detection scope ranging from 0.1 to 2000 μM and excellent selectivity. The as-prepared Cys-Au NCs/Fe^{3+} was demonstrated to be an ultrasensitive and selective nanoprobe for the detection of ascorbic acid. This study indicated that the "on–off–on" fluorescent probes Cys-Au NCs held a promising application for the bidirectional detection of Fe^{3+} and ascorbic acid. Furthermore, our novel "on–off–on" fluorescent probes provided insight into the rational design of thiolate-protected gold nanoclusters for biochemical analysis of high selectivity and sensitivity.

Received 19th January 2023
Accepted 15th February 2023

DOI: 10.1039/d3ra00410d

rsc.li/rsc-advances

1. Introduction

The advent of nanomaterials has significantly impacted the landscape of life science research, opening new avenues for exploration and expanding the boundaries of conventional thinking. The use of traditional fluorescent nanomaterials such as organic fluorescent dyes,[1–3] fluorescent proteins,[4–6] and quantum dots[7–10] in life science research has become widespread, however, they are limited by several inherent limitations. For instance, organic fluorescent dyes exhibit a short Stokes shift, poor photochemical stability, sensitivity to buffer composition (which can result in quenching or decomposition due to pH changes), and high susceptibility to photobleaching and decomposition upon repeated excitation.[11] On the other hand, while fluorescent proteins hold promise, they are not widely used due to factors such as slow maturation, a tendency to polymerize, and the potential for toxicity to cells.[12] Furthermore, the fluorescence time after being excited is also limited.[13] Although quantum dots have many excellent fluorescence properties, such as better photostability, a large Stokes shift, wide excitation spectrum, adjustable emission wavelength, and narrow and symmetrical spectrum, which can achieve "one excitation, multiple emission[14]" and many other advantages, they also has some inherent disadvantages, such as the large size, the presence of toxic elements, and the blinking phenomenon. In light of these limitations, metal nanoclusters have gained increasing attention as an alternative to traditional fluorescent nanomaterials due to their small size, stable and tunable fluorescence properties,[15] low toxicity, good biocompatibility, and easy and economical preparation process.[16]

Fluorescent gold nanoclusters, also known as gold clusters,[17] represent a new type of fluorescent nanomaterial and offer unique fluorescent properties compared to traditional fluorescent dyes, such as good photostability, small size, large Stokes shift, absence of flickering phenomenon, and large cross-sectional area of two-photon absorption. Furthermore, the absence of toxic metal elements and good biocompatibility make them suitable for a broad range of applications in the biological field.[18–20] In recent years, the study of luminescent gold nanoclusters has emerged as a research hotspot in both materials science and life science and has demonstrated broad applications in areas such as biosensing,[21–23] optical imaging,[24–26] drug delivery,[27,28] and tumor therapy.[29]

Therefore, in this study, we reported a novel fluorescent probe Cys-Au NCs, prepared by decomposing Au(I)–thiolate complexes. It exhibited stable red-orange fluorescence

[a]*Department of Pharmacy, Xiangyang No.1 People's Hospital, Hubei University of Medicine, Xiangyang, 441000, China*

[b]*Department of Pharmacy, Taihe Hospital, Hubei University of Medicine, Shiyan, 442000, China*

[c]*Department of Anesthesiology, Xiangyang Key Laboratory of Movement Disorders, Xiangyang No.1 People's Hospital, Hubei University of Medicine, Xiangyang, 441000, China. E-mail: 603983267@qq.com*

† Electronic supplementary information (ESI) available. See DOI: https://doi.org/10.1039/d3ra00410d

‡ Wenjie Luo and Changxu Wang contributed equally to the work and should be regarded as co-first authors.

emission at 570 nm. Moreover, the fluorescence intensity was significantly lower by the addition of ferric ions due to IFE. However, when ascorbic acid was added to the quenching solution, the fluorescence of Cys-Au NCs recovered. This fluorescence recovery phenomenon could be attributed to the redox reaction that occurred between Fe^{3+} and ascorbic acid. Cys-Au NCs could detect Fe^{3+} and ascorbic acid content bi-directionally *via* an "on–off–on" fluorescence mode as novel sensors in the application of other biological and environmental detection.

2. Experimental section

2.1 Reagents

All chemical reagents are of analytical or higher grade and used without further purification. Cysteine (Cys), cystine, L-glutathione (reduced type, GSH), *N*-acetyl-L-cysteine (NAC), penicillamine (DPA), phenylalanine (Phe), glycine (Gly), glutamic acid (Glu), aspartic acid (Asp), methionine (Met), cystine (Cys–Cys), *N*-acetyl-L-cysteine (Hcy), glutathione (GSH), ascorbic acid (AA) and citric acid (CA) were obtained from Aladdin (Shanghai, China). Chloroauric acid ($HAuCl_4$) was provided by Sigma Aldrich Trading Ltd. Metal ions were purchased by Sinopharm Chemical Reagent Co., Ltd (Shanghai, China). Vitamin C tablets (Vifuga) were taken from the Taihe Hospital (Hubei, China). Ultra-pure water (Milli-Q 18.2 MΩ cm) was produced using a water filtration system (Millipore, Biocel).

2.2 Instrumentations

Transmission electron microscope (TEM) images of Cys-Au NCs were performed by transmission electron microscope (Talos f200s, FEI, USA). The size distribution was determined by size analyzer (ZEN3690, Malvern Instruments Ltd, UK). Fluorescence spectra were recorded with an F-7000 spectrophotometer (Hi-Tech Co., Ltd, Japan). The UV-vis absorption spectra were obtained with a UV-2600 spectrophotometer (Shimadzu Co., Japan). X-ray photoelectron spectra (XPS) were measured with an ESCALAB 250Xi electron spectrometer (Thermo Fisher Scientific, Inc., USA).

2.3 Preparation of Cys-Au NCs

Compared with the previous work, we proposed a different approach which can be used to synthesis Cys-Au NCs with high fluorescence emission. Firstly, $HAuCl_4$ (20 mM, 100 μL) was added to 1.8 mL of ultra-pure water with gentle agitation at 25 °C. A freshly prepared aqueous solution of Cys (100 mM, 0.3 mL) was then added to the reaction system and when the light yellow solution became colorless, 100 equivalents of hydrochloric acid (200 μL of 1 M HCl) was introduced. After that, the mixture was heated to 40 °C under mild stirring for 1.5 hours and then centrifuged at 6000 rpm for 3 minutes in a TG-16-II centrifuge. Afterwards, the centrifugates were purified using aqueous washing and then dispersed in ultrapure water (pH = 6.5). Finally, the purified Cys-Au NCs solution was stored at 4 °C for further use.

2.4 Detection of Fe^{3+} and ascorbic acid using Cys-Au NCs

For detection of Fe^{3+}, the $FeCl_3 \cdot 6H_2O$ was used to prepare Fe^{3+} stock solution (10 mM). We diluted the stock solution with ultrapure water to obtain various concentrations of ferric ion solutions (0.1, 0.2, 0.3, 0.4, 0.5, 10, 50, 100, 150, 250, 500, 800, 1000, 1500, 2000 μM). The Cys-Au NCs solution was diluted to a concentration of 0.167 mM and then mixed with different concentrations of Fe^{3+} solutions in equal volumes. Finally, the fluorescence emission spectra were observed and recorded with excitation at 365 nm after mixing for ten minutes.

For the detection of ascorbic acid, 100 μL of Fe^{3+} solution (final concentration of 0.5 mmol L^{-1}) was introduced to 100 μL of Cys-Au NCs/Fe^{3+} suspension (30 mg L^{-1}) for the formation of a sensitive and selective fluorescent probe, represented as Cys-Au NCs/Fe^{3+}. 100 μL of ascorbic acid solution at different concentrations was then added under homogeneously stirring. After 10 min at room temperature, the fluorescence data were recorded by F-7000 spectrophotometer. The selectivity of the Cys-Au NCs/Fe^{3+} probe for ascorbic acid was tested *via* the introduction of other interfering substances, including phenylalanine (Phe), glycine (Gly), glutamic acid (Glu), aspartic acid (Asp), penicillamine (DPA), methionine (Met), cystine (Cys–Cys), L-cysteine (L-Cys), *N*-acetyl-L-cysteine (Hcy), glutathione (GSH) and citric acid (CA).

2.5 Analysis of human serum samples

Serum samples, from ten healthy adult volunteers who had provided informed consent, were collected by the Laboratory Department of Xiangyang No.1 Peoples' Hospital of Hubei Province, China. These samples were then pre-treated according to published procedures.[30,31] The procedure was shown below: 1.0 mL of ultrapure water was added to 0.5 mL of serum sample and mixed, then shaken and added to trichloroethanol solution (20%, 1.0 mL). The solution was shaken and mixed for 45 minutes, then the protein was separated by centrifugation at 130 000 rpm to obtain the supernatant. Afterwards, 5 μL of 3% H_2O_2 solution was introduced to 1.0 mL of supernatant to oxidize Fe^{2+} to Fe^{3+} for fluorescence detection, and each sample was measured three times. Finally, the Fe^{3+} concentration in the serum samples was calculated from the measured fluorescence intensity and regression curves.

2.6 Determination of ascorbic acid in vitamin C

20 vitamin C tablets samples were randomly taken in a mortar, fully crushed. Then accurately weighed 0.0250 g sample powder was placed in a beaker, dissolved in 2 mL of 10% acetic acid, and transferred to a 100 mL brown volumetric flask. In addition, the volume was fixed with ultrapure water, shaken well and filtered. Lastly, 1.00 mL of vitamin C tablet sample solution was pipetted for testing. Each sample was measured three times and the concentration of AA was calculated from the measured fluorescence intensity and the regression curve.

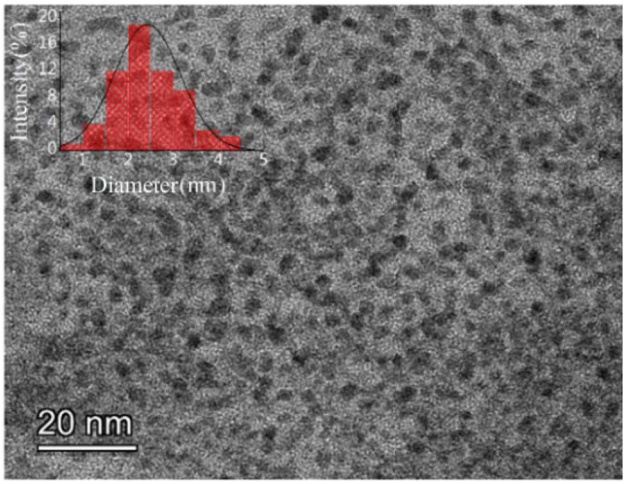

Fig. 1 TEM image of Cys-Au NCs; the inset shows the size distribution. Scale bar: 20 nm.

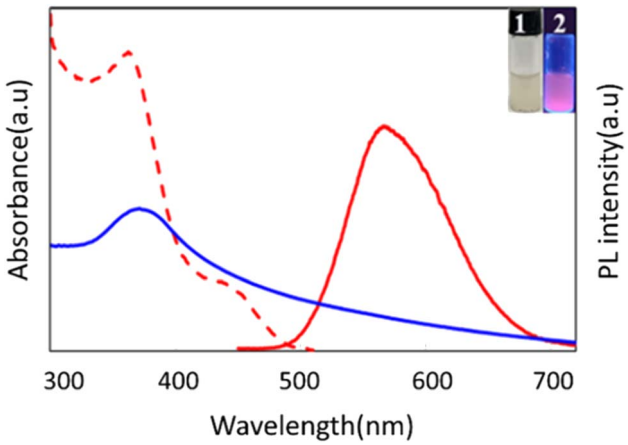

Fig. 2 UV absorption (blue solid line), emission spectrum (red solid line, $\lambda_{ex} = 365$ nm) and excitation spectrum (red dotted line, $\lambda_{em} = 570$ nm) of Cys-Au NCs. (Inset) Images of Cys-Au NCs in (1) visible light and (2) UV light.

3. Results and discussion

3.1 Characterization of Cys-Au NCs

The morphology and size distribution of the prepared fluorescent Cys-Au NCs were examined and characterized by transmission electron microscopy and dynamic light scattering, respectively. As shown in Fig. 1, TEM results demonstrated that the morphology of Cys-Au NCs was homogeneous with an average size of 2.43 nm, while DLS indicated that the hydrodynamic diameter of Cys-Au NCs was 193.9 nm (Fig. S1†). However, the dimensional results measured using TEM were significantly smaller than those of DLS. In non-basic solutions, –[Cys-Au(I)]$_n$-polymers might self-assemble into –[Cys-Au(I)]$_n$-polymers with random morphology and diameters higher than 100 nm *via* superimposed hydrogen bonding and zwitterionic effects between Cys ligands and *via* the lipophilic interaction of Au(I)···Au(I).[32]

The optical properties of the synthesized Cys-Au NCs were characterized by UV-vis and fluorescence spectroscopy. It could be seen from Fig. 2 that the Cys-Au NCs showed a UV absorption peak at 380 nm, which was similar to the Cys-Au NCs synthesized in the relevant reported literature.[33] The intense absorption band at 380 nm could be attributed to ligand-to-metal charge transfer (LMCT; S → Au) and ligand charge transfer between metals (LMMCT; S → Au–Au), which was a characteristic transition of supramolecular gold compounds and gold clusters. As Cys-Au NCs exhibited a high gold oxidation state, there was a lack of free electrons to generate coherent oscillations.[34] Thus, it showed no resonant absorption of the surface plasma of the gold nanoparticles at 520 nm in the UV spectrum. Meanwhile, under UV irradiation (365 nm), the Cys-Au NCs fluoresced bright red-orange with a quantum yield (QY) of approximately 4.41% calibrated with quinine sulphate. When the excitation and emission peaks were at 360 nm and 570 nm, respectively, the fluorescence of Au NCs was produced by ligand-metal charge transfer between the thiol salt and Au NCs.[35] According to the study before,[35] the mechanism behind the fluorescence of Cys-Au NCs was the generation of Au(0) core through the decomposition reaction of Au(I)–thiolate complexes with hydrochloric acid. The Au(I)–thiolate complexes then aggregated on the generated Au(0) *in situ*, forming nanoclusters with a strong fluorescent core–shell structure, thus emitting a stable red-orange fluorescence at 570 nm.

To investigate the elemental composition and valence of the clusters, we tested the X-ray photoelectron spectra of Cys-Au NCs. As shown in Fig. S2a,† the binding energy of Au atoms in Cys-Au NCs was 84.6 eV at the Au ($4f_{7,2}$) orbital, located between 84.0 eV for Au (0) and 86.0 eV for Au(I), which indicated that both Au(I) and Au (0) were present in the gold cluster. According to the data fitting, the percentage of Au (0) and Au(I) was 19% and 81% respectively. Meanwhile, the core level spectra of C (1s), O (1s), N (1s) and S (2p) evidenced the presence of the protecting Cys ligands (Fig. S2b†).

3.2 Cys-Au NCs for the detection of Fe^{3+}

To study the specificity of the synthesized Cys-Au NCs for certain metal ions, the fluorescent probes were tested in response to other common metal cations (Ag^+, Al^{3+}, Ba^{2+}, Ca^{2+}, Co^{2+}, Cr^{3+}, Cu^{2+}, Fe^{2+}, Fe^{3+}, Mg^{2+}, Mn^{2+}, Ni^{2+}, Pb^{2+}, Sn^{2+}, Sr^{2+}, Zn^{2+}) for 3 minutes and then the change of fluorescence intensities were measured. As shown in Fig. S3a,† a sharp decrease in fluorescence intensity could be induced by Fe^{3+} only. Meanwhile, no significant fluorescence shift was noticed in the absence of other cations, indicating that the Cys-Au NCs probe was highly selective for ferric ions. Accordingly, experimental results illustrated that Cys-Au NCs could be rapidly synthesized by a simple preparation process and that their good dispersibility and biocompatibility allowed for Fe^{3+} detection with high selectivity in complex environments.

To further explored the practicality and utility of this fluorescent probe, anti-interference experiments were conducted. A variety of ten-fold concentrations of metal ions were added to the fluorescent probe Cys-Au NCs, followed by the addition of

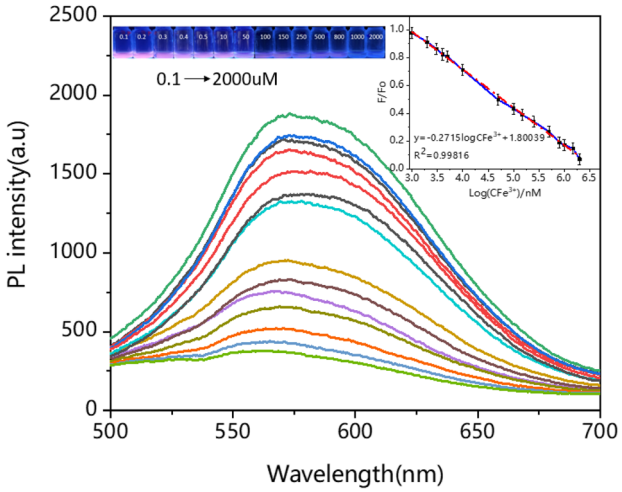

Fig. 3 Fluorescence response of Cys-Au NCs solutions with different concentrations of Fe^{3+}. Right inset: standard curve for the determination of Fe^{3+} concentration. Left inset: Cys-Au NCs under UV light with different concentrations of Fe^{3+} in the range from 0.1 to 2000 μM.

Fe^{3+} for fluorescence testing. A comparison of the changes in fluorescence intensity in Fig. S3b† illustrated that the fluorescent probe Cys-Au NCs, unaffected by other interfering ions, had a favorable anti-interference ability for the selective detection of ferric ions. Therefore, this fluorescent probe could be applied as a probe for the identification of Fe^{3+} in complicated environmental samples.

In addition, further studies were carried out on the fluorescence probes. Fig. 3 displayed the fluorescence spectra of Cys-Au NCs in different concentrations of (0.1, 0.2, 0.3, 0.4, 0.5, 10, 50, 100, 150, 250, 500, 800, 1000, 1500, 2000 μM) Fe^{3+} at pH 6.5. It could be noticed that with the increase of Fe^{3+} concentration, the corresponding fluorescence intensity gradually decreased. When the concentration reached 2000 μM, the degree of fluorescence quenching was 91.67%. Right inset of Fig. 3 showed the linear curve plotted with Fe^{3+} concentration as abscissa and fluorescence quenching efficiency (F/F_0) as ordinate. According to the results, we obtained a well-fitting regression curve between the logarithm of the Fe^{3+} concentration and the fluorescence intensity ratio (570 nm) in the range of 0.1 μM to 2000 μM, $F/F_0 = -0.2715 \log C_{Fe^{3+}} + 1.80039$ ($R^2 = 0.998$), $F_0 = 7612 > F_{0.05}(1, 12) = 4.747$, as shown by the F-test: the linear relationship between X and Y was significant. The relative standard deviation (RSD) of Cys-Au NVs was 0.12% with good linearity over the range of 0.1 μM to 2000 μM. As important analytical parameters, the limit of detection (LOD) and limit of quantification (LOQ) were calculated by $3\sigma/k$ and $10\sigma/k$ ($3\sigma/k$, σ is the standard deviation of multiple measurements of a blank sample, and K is the slope of the equation) for Cys-Au NCs of 11 nM and 37 nM (Fig. S4 and Table S1†). The confidence intervals for LOD and LOQ of Cys-Au NCs were 11–14 nM and 36–47 nM, respectively. The LOD was obviously lower than most of the previously reported assays based on Au NCs for Fe^{3+} detection, as shown in Table S2.†

3.3 The fluorescence quenching mechanism of Cys-Au NCs

We investigated the fluorescence quenching mechanism of Cys-Au NCs in the presence of Fe^{3+}. The Cys-Au NCs could be quenched by Fe^{3+} with no fluorescence at 365 nm of UV. There was no overlap between the Fe^{3+} absorption and emission spectra of the Cys-Au NCs, as shown in Fig. 4a, and resonance energy transfer (RET) was ruled out. In contrast, Fe^{3+} has a strong absorption spectrum between 260 and 400 nm, which overlaps with the excitation peak of Cys-Au NCs at 365 nm, indicating that the quenching was caused by the inner filter effect (IFE).[36]

Relative to the high selectivity of Cys-Au NCs for Fe^{3+}, we hypothesized that the fluorescence of Cys-Au NCs would be restored when Fe^{3+} was reduced to Fe^{2+}. To test the hypothesis, ascorbic acid was selected to reduce Fe^{3+} to Fe^{2+}, as shown in Fig. S5.† Ascorbic acid can reduce Fe^{3+} to Fe^{2+}, and the reduction product Fe^{2+} has no significant effect on the fluorescence

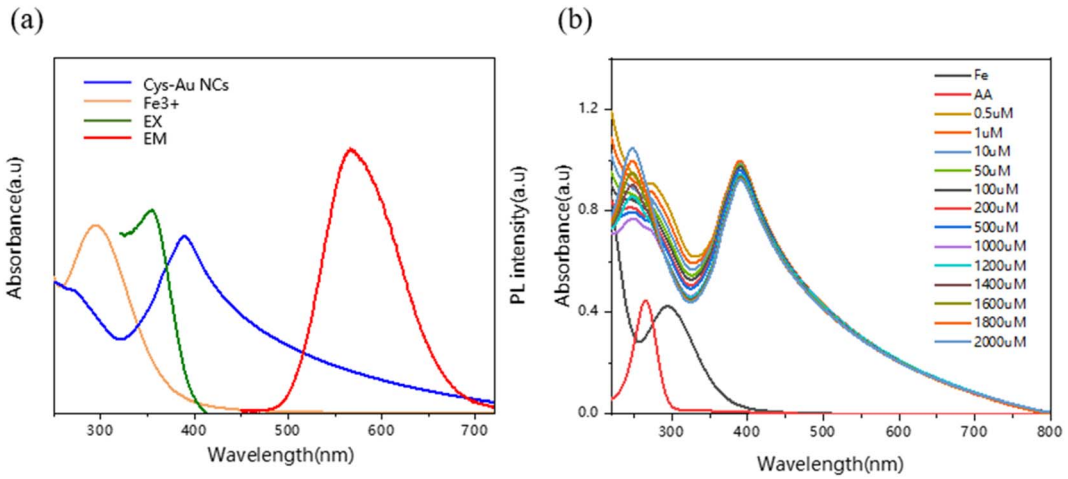

Fig. 4 (a) UV-vis absorption (blue line), excitation (olive line), and emission (red line) spectra of Cys-Au NCs, and UV-vis absorption spectral lines of Fe^{3+} ions (500 μM, orange line). (b) UV-vis absorption spectrum of Cys-Au NCs/Fe^{3+} with the addition of ascorbic acid.

intensity of Cys-Au NCs. When only ascorbic acid was added to the Cys-Au NCs system, there was no significant change in fluorescence intensity as shown by the blue line in Fig. S6a,† indicating that ascorbic acid had no effect on the probe Cys-Au NCs. However, the fluorescence of composite Cys-Au NCs/Fe^{3+} could be effectively restored after the addition of ascorbic acid. The UV absorption spectra of the fluorescent probe Cys-Au NCs, as shown in Fig. S6b† and 4b, were not red-shifted or blue-shifted during the fluorescence quenching or recovery processes, indicating that the fluorescent probe's structure was not damaged. In conclusion, the principle that Fe^{3+} destroyed the structure of the fluorescent probe Cys-Au NCs *via* a redox mechanism to achieve fluorescence quenching could be rejected, demonstrating that the generation of IFE between Cys-Au NCs and Fe^{3+} resulted in fluorescence quenching.

3.4 Cys-Au NCs/Fe^{3+} for the detection of ascorbic acid

Based on the bidirectional principle of complex-dissociation, we evaluated whether Cys-Au NCs/Fe^{3+} could be used as a fluorescent probe for the detection of ascorbic acid. Hence, selectivity experiments were carried out to assess the potential application of Cys-Au NCs/Fe^{3+} composite. Under the same experimental conditions, potential interfering substances (Phe, Gly, Glu, Asp, DPA, Met, Cys–Cys, L-Cys, NAC, GSH, CA) had no noticeable effect on the fluorescence intensity of Cys-Au NCs/Fe^{3+}. Even for the bioreductase GSH, there was still no apparent effect on the detection of ascorbic acid. As shown in Fig. S7,† this fluorescent probe was highly selective, which could provide a solid foundation for its practical applications.

As shown in Fig. 5, as the concentration of AA increased, the corresponding fluorescence intensity gradually expanded. The highest fluorescence intensity was achieved when the AA concentration was 1000 μM, reaching almost 99.9% of the original solution. When the AA concentration continued to increase, there was no enhancement in fluorescence intensity. The figure on the right showed a linear curve with a linear range of 0.1 to 1000 μM and a linear equation of $F/F_0 = 0.21097 \log C_{AA} - 0.40038$ ($R^2 = 0.98557$), $F_0 = 1574 > F_{0.05}$ (1, 6) = 5.987, as shown by the *F*-test: the linear relationship between *X* and *Y* was significant. The limit of detection (LOD) and limit of quantification (LOQ) of Cys-Au NCs/Fe^{3+} were calculated by $3\sigma/k$ and $10\sigma/k$ ($3\sigma/k$, σ is the standard deviation of multiple measurements of a blank sample, and *K* is the slope of the equation) for Cys-Au NCs/Fe^{3+} of 14 nM and 47 nM (Fig. S8 and Table S3†). The Cys-Au NCs/Fe^{3+} was of higher sensitivity compared to conventional detection methods, as shown in Table S4.† Overall, based on the high sensitivity and selectivity of the material and the good linear regression, the "on–off–on" fluorescent probes Cys-Au NCs had promising applications for the bidirectional detection of Fe^{3+} and ascorbic acid.

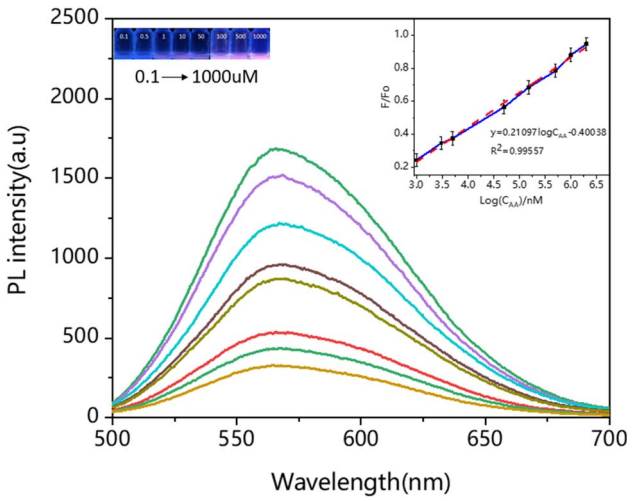

Fig. 5 Fluorescence response of different concentrations of ascorbic acid with Cys-Au NCs/Fe^{3+}. Right inset: standard curve for the determination of ascorbic acid concentration. Left inset: Cys-Au NCs/Fe^{3+} under UV light with different concentrations of AA in the range from 0.1 to 1000 μM.

3.5 Quantitative determination of Fe^{3+} in serum samples

Some clinical disorders, such as anaemia and acute leukaemia, demand a serum iron level for diagnosis.[37,38] The fluorescent probe Cys-Au NCs had potential for application in serum iron determination due to its sensitive and selective response to ferric ions. To verify the practicality of this method, ten serum samples from volunteers were tested during the treatment and the results are shown in Table 1. We separated the ferric ions from the protein by trichloroacetic acid (20%), and oxidized Fe^{2+} to Fe^{3+} under the presence of hydrogen peroxide (H_2O_2). The pretreated serum was then mixed with the fluorescent probe Cys-Au NCs and the fluorescence intensity was measured after 3 minutes of incubation. Assays were performed in triplicate for each group, and the average was obtained while the relative standard deviation (RSD) was calculated. At the same time, the spiked recovery of the samples was determined.

A serum iron assay kit (colorimetric method) was known to be used in hospitals. This method was based on the principle that serum iron was rapidly lysed from serum proteins under the action of nonionic surfactants and iron dissociation agent, and reduced to Fe^{2+}. The purple compound, formed by the reaction of Fe^{2+} with ferrous zine, could be determined colorimetrically by absorbance analysis at 562 nm by spectrophotometer and with a recovery of 98.4%. By comparing the results of our measurements with the serum iron test report, the fluorescent probe Cys-Au NCs were confirmed to be applicable for serum iron determination. Simultaneously, the recovery ranged from 93.97% to 112.79% with an RSD of 0.63 to 1.59% ($n = 3$). According to the *F*-test, there was no significant difference in precision between the two methods, and t (0.037) was less than the critical value $t_{0.05,18}$ (2.101) at 95% confidence level, which indicated that there was no significant difference in the values of our method compared to the conventional method for the determination of serum iron content. The materials used in this method were not only simple to synthesize, but also showed stable performance. It was however more sensitive than the ferrous zine spectrophotometric method used in conventional serum iron assays. In addition, the method had the advantages of less serum consumption, rapid and simple operation,

Table 1 Iron content of serum samples

Volunteer serum	Iron content (μmol L^{-1})	Standard value (μmol L^{-1})	RSD (%, $n = 3$)	Recovery (%, $n = 3$)
Sample 1	10.85	9.62	1.59	112.79
Sample 2	30.77	32.78	0.63	93.97
Sample 3	16.83	15.43	1.04	109.07
Sample 4	20.71	20.53	0.46	100.88
Sample 5	33.23	34.61	0.87	96.01
Sample 6	17.45	17.28	0.97	100.98
Sample 7	16.02	15.67	0.84	102.23
Sample 8	25.38	24.32	1.21	104.36
Sample 9	22.32	22.55	0.89	98.98
Sample 10	36.45	35.78	1.12	96.16

Table 2 AA content of vitamin C tablets

Number	Measured values[a] (mg per tablet)	Measured values (pharmacopoeia method)[a] (mg per tablet)	RSD (%, $n = 3$)	Recovery (%, $n = 3$)
1	98.2	98.4	0.17	99.80
2	97.8	97.9	0.94	99.90
3	98.5	98.2	0.52	100.31
4	97.6	97.3	0.83	100.30
5	98.1	98.2	0.28	99.90
6	98.3	97.9	0.65	100.41

[a] Mean value ± standard deviation ($n = 3$).

sensitive and reliable results, and was more suitable for clinical application.

3.6 Determination of ascorbic acid in vitamin C

The concentration of ascorbic acid in the diluted solution was calculated according to the measured fluorescence intensity and the regression curve, and then compared with the iodometric method specified in the Chinese Pharmacopoeia (2020). The results in the Table 2 indicated that there was no significant difference between the results of this method and the standard method (Pharmacopoeia method) at the 95% confidence level by *t*-test, t (0.481) is less than the critical value $t_{0.05,10}$ (2.228). Thus, our fluorescence probe also had potential in the field of bioanalysis for the detection of ascorbic acid in practical samples.

4. Conclusion

In summary, an "on–off–on" fluorescent switching nanoprobe, synthesized by the decomposition of Au(I)–thiolate complexes, was developed for the selective detection of Fe^{3+} and ascorbic acid. The experimental data implicated that the iron and ascorbic acid concentrations in real samples could be determined respectively using Cys-Au NCs with good linear regression and high sensitivity in comparison of conventional approach. Therefore, this novel fluorescent probe could be expected to provide a sensitive platform for rapid quantitative detection. Meanwhile, this also broadened application potential to various fields like the design of fluorescent probes and biochemical analysis.

Conflicts of interest

There are no conflicts to declare.

References

1 A. S. Ethiraj, N. Hebalkar, S. Kharrazi, J. Urban, S. R. Sainkar and S. K. Kulkarni, *J. Lumin.*, 2005, **114**, 15–23.
2 H. H. Pham, I. Gourevich, J. K. Oh, J. E. Jonkman and E. Kumacheva, *Adv. Mater.*, 2004, **16**, 516–520.
3 J. Yan, M. C. Estévez, J. E. Smith, K. Wang, X. He, L. Wang and W. Tan, *Nano today*, 2007, **2**, 44–50.
4 B. T. Bajar, E. S. Wang, S. Zhang, M. Z. Lin and J. Chu, *Sensors*, 2016, **16**, 1488.
5 V. Sample, R. H. Newman and J. Zhang, *Chem. Soc. Rev.*, 2009, **38**, 2852–2864.
6 A. Miyawaki, *Annu. Rev. Biochem.*, 2011, **80**, 357–373.
7 S. Tajik, Z. Dourandish, K. Zhang, H. Beitollahi, Q. Van Le, H. W. Jang and M. Shokouhimehr, *RSC Adv.*, 2020, **10**, 15406–15429.
8 M. Li, T. Chen, J. J. Gooding and J. Liu, *ACS Sens.*, 2019, **4**, 1732–1748.
9 M. J. Molaei, *Talanta*, 2019, **196**, 456–478.
10 C. T. Matea, T. Mocan, F. Tabaran, T. Pop, O. Mosteanu, C. Puia, C. Iancu and L. Mocan, *Int. J. Nanomed.*, 2017, **12**, 5421.

11 A. Auger, J. Samuel, O. Poncelet and O. Raccurt, *Nanoscale Res. Lett.*, 2011, **6**, 1–12.
12 M. V. Matz, A. F. Fradkov, Y. A. Labas, A. P. Savitsky, A. G. Zaraisky, M. L. Markelov and S. A. Lukyanov, *Nat. Biotechnol.*, 1999, **17**, 969–973.
13 W. Tao, B.-G. Evans, J. Yao, S. Cooper, K. Cornetta, C. B. Ballas, G. Hangoc and H. E. Broxmeyer, *Stem Cells*, 2007, **25**, 670–678.
14 S. Wang, A. Clapper, P. Chen, L. Wang, I. Aharonovich, D. Jin and Q. Li, *J. Phys. Chem. Lett.*, 2017, **8**, 5673–5679.
15 S. Maity, D. Bain and A. Patra, *Nanoscale*, 2019, **11**, 22685–22723.
16 N. Goswami, Q. Yao, T. Chen and J. Xie, *Coord. Chem. Rev.*, 2016, **329**, 1–15.
17 Q. Zhang, J. Xie, Y. Yu and J. Y. Lee, *Nanoscale*, 2010, **2**, 1962–1975.
18 Z. Liu, Z. Wu, Q. Yao, Y. Cao, O. J. H. Chai and J. Xie, *Nano Today*, 2021, **36**, 101053.
19 X. Qu, Y. Li, L. Li, Y. Wang, J. Liang and J. Liang, *J. Nanomater.*, 2015, **2015**, 4.
20 L. Zhang and E. Wang, *Nano Today*, 2014, **9**, 132–157.
21 T. W. Clarkson and L. Magos, *Crit. Rev. Toxicol.*, 2006, **36**, 609–662.
22 C.-C. Huang, Z. Yang, K.-H. Lee and H.-T. Chang, *Angew. Chem.*, 2007, **119**, 6948–6952.
23 X. Yuan, Z. Luo, Y. Yu, Q. Yao and J. Xie, *Chem.–Asian J.*, 2013, **8**, 858–871.
24 L. Shang, R. M. Dörlich, S. Brandholt, R. Schneider, V. Trouillet, M. Bruns, D. Gerthsen and G. U. Nienhaus, *Nanoscale*, 2011, **3**, 2009–2014.
25 A. Retnakumari, S. Setua, D. Menon, P. Ravindran, H. Muhammed, T. Pradeep, S. Nair and M. Koyakutty, *Nanotechnology*, 2009, **21**, 055103.
26 X. Wu, X. He, K. Wang, C. Xie, B. Zhou and Z. Qing, *Nanoscale*, 2010, **2**, 2244–2249.
27 T. Chen, S. Xu, T. Zhao, L. Zhu, D. Wei, Y. Li, H. Zhang and C. Zhao, *ACS Appl. Mater. Interfaces*, 2012, **4**, 5766–5774.
28 Y. Zhang, J. Li, H. Jiang, C. Zhao and X. Wang, *RSC Adv.*, 2016, **6**, 63331–63337.
29 H. Kawasaki, S. Kumar, G. Li, C. Zeng, D. R. Kauffman, J. Yoshimoto, Y. Iwasaki and R. Jin, *Chem. Mater.*, 2014, **26**, 2777–2788.
30 X. Mu, L. Qi, P. Dong, J. Qiao, J. Hou, Z. Nie and H. Ma, *Biosens. Bioelectron.*, 2013, **49**, 249–255.
31 A. Yilmaz, Y. Ensari, B. Otludil, M. Sabri Batun, R. Longo and L. Dalla Palma, *Phys. Med.*, 1990, **6**, 237–238.
32 J. Li, M. Huo, J. Wang, J. Zhou, J. M. Mohammad, Y. Zhang, Q. Zhu, A. Y. Waddad and Q. Zhang, *Biomaterials*, 2012, **33**, 2310–2320.
33 Y. S. Borghei, M. Hosseini and M. R. Ganjali, *Sens. Actuators, B*, 2018, **273**, 1618–1626.
34 P. K. Jain, K. S. Lee, M. A. El-Sayed and I. H. El-Sayed, *J. Phys. Chem. B*, 2006, **110**, 7238–7248.
35 Z. Wu and R. Jin, *Nano Lett.*, 2010, **10**, 2568–2573.
36 L. Guo, Y. Liu, R. Kong, G. Chen, Z. Liu, F. Qu, L. Xia and W. Tan, *Anal. Chem.*, 2019, **91**, 12453–12460.
37 T. Fujita, H. Hamasaki, C. Furukata and M. Nonobe, *Clin. Chem.*, 1994, **40**, 763–767.
38 B. Klein, N. Kleinman and R. L. Searcy, *Clin. Chem.*, 1970, **16**, 495–499.